240 GHz pedestal-free colliding-pulse mode-locked laser with a wide operation range

2014 Laser Phys. Lett. 11 115804

(http://iopscience.iop.org/1612-202X/11/11/115804)

OPEN ACCESS
IOP Publishing | Astro Ltd
Laser Physics Letters
Laser Phys. Lett. **11** (2014) 115804 (5pp)
doi:10.1088/1612-2011/11/11/115804

240 GHz pedestal-free colliding-pulse mode-locked laser with a wide operation range

L Hou, M Haji and J H Marsh

School of Engineering, University of Glasgow, Glasgow, G12 8LT, UK

E-mail: lianping.hou@glasgow.ac.uk

Received 22 April 2014, revised 13 August 2014
Accepted for publication 14 August 2014
Published 19 September 2014

Abstract

A 240 GHz, sixth-harmonic monolithic ~1.55 μm colliding-pulse mode-locked laser is reported using a three-quantum-well active layer design and a passive far-field reduction layer. The device emits 0.88 ps pulses with a peak power of 65 mW and intermediate longitudinal modes suppressed by >30 dB. The device demonstrates a wide operation range compared to the conventional five-quantum-well design as well as having a low divergence angle (12.7° × 26.3°), granting a twofold improvement in butt-coupling efficiency into a flat cleaved single-mode fibre.

Keywords: AlGaInAs, harmonics, mode locked laser, optical pulse generation

(Some figures may appear in colour only in the online journal)

1. Introduction

Cheap, compact and reliable 1.55 μm wavelength semiconductor mode-locked lasers (MLLs) with a 240 GHz pulse repetition rate operating with high power and a wide operation range are highly desirable for ultrahigh bit-rate time-division multiplexed (TDM) optical networks, high speed signal processing and wireless transmission of multi-channel non-compressed high definition television signals due to the pulse repetition frequency being located in one of the atmospheric windows. Recently, 1.55 μm quantum-well (QW) and quantum-dash MLLs with short cavity lengths have been demonstrated with pulse repetition frequencies >100 GHz [1, 2]. However, the output power from short cavity length devices is limited by thermal and gain saturation effects. Greater pulse-repetition rates can be achieved with a longer cavity using harmonic mode-locking (ML) techniques, and one way to realize this is to use the colliding-pulse ML (CPM) configuration [3–5]. The monolithic CPM laser is a compact light source which is thermally and mechanically very stable, and can be made using relatively simple fabrication processes, while having less stringent cleaving tolerances compared with the compound-cavity design [6].

In order to increase the average output power of CPM lasers without increasing the duration of the pulses, an epitaxial design was developed with a smaller number of QWs [7, 8] resulting in reduced internal losses (α_i) and a high saturation energy ($E_{sat} = h\nu A/(\Gamma \mathrm{d}g/\mathrm{d}N)$, where $h\nu$ is the photon energy, A is the mode area, $\mathrm{d}g/\mathrm{d}N$ is the differential gain, and Γ is the optical confinement factor). Fewer QWs result in a reduction of α_i, Γ and $\mathrm{d}g/\mathrm{d}N$, and thus provides a higher E_{sat} which is essential to deliver stable ML operation [8]. In order to further increase the average output power whilst enlarging the range of bias parameters to enable ML without increasing the pulse pedestal, the modal area A should be increased, which will naturally decrease the value of α_i and Γ, and increase the value of E_{sat}. This also has the benefit of reducing the angular spread of the far-field pattern (FFP), enabling a simplified, and high-yield optical alignment when used in practical applications.

In this work, we have used the epitaxial laser structure previously reported in [9]. The active region has three 6 nm thick compressively-strained (+1.2%) AlGaInAs QWs and four 10 nm thick tensile-strained (−0.3%) AlGaInAs quantum-barriers. The design incorporates a 160 nm thick 1.1Q ($In_{0.85}Ga_{0.15}As_{0.33}P$) far-field reduction layer (FRL). Due to the finite carrier recovery time, an increase of the ML frequency or a reduction of the pulse width is often accompanied by the formation of pulse pedestals. These pedestals cause degradation in the signal to noise ratio and increased timing jitter. By using an AlGaInAs active layer, we have reduced the recovery time

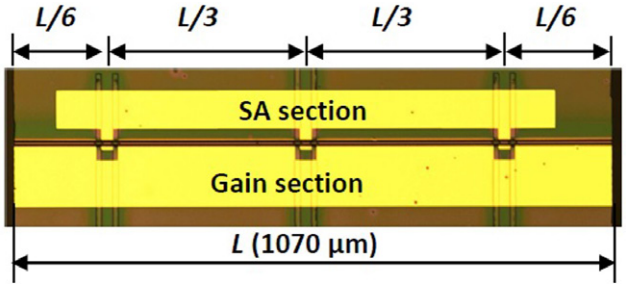

Figure 1. Optical microscope picture of the 240 GHz CPM device (top view) indicating its dimensions and the positions of the three SA sections.

to <5 ps [10], achieving exceptional mode-locking characteristics with a negligible pedestal at 240 GHz. The low Γ value (2.19%) brings the following benefits: (1) reduced coupling of amplified spontaneous emission (ASE), (2) a reduction in self-phase modulation (SPM), (3) reduced waveguide dispersion [11], and (4) a low α_i (8 cm^{-1}). These benefits along with the increased spot size and long cavity (1070 μm) enable the laser to operate with a high output power and stable short pulse ML operation over a wide range of drive parameters.

By fabricating devices with the sixth-harmonic CPM configuration described in [5], we have developed a 240 GHz CPM laser operating at 1.55 μm. We show that the three-QW based design has a substantially wider operation range than the equivalent and conventional five-QW based counterpart. Furthermore, we present a comprehensive mapping of the ML regions as a function of the applied drive parameters.

2. Device structure and fabrication

The fabricated devices have a total length (L) of 1070 μm, three 20 μm long saturable absorbers (SAs) located as shown in figure 1, i.e. one SA located in the middle of the cavity, and the other two SAs located at L/6 from each of the facets. Such a configuration supports ML at the sixth harmonic [5]. The three SAs were electrically connected using a single contact. The remaining four sections were also electrically connected using a single contact (figure 1) and forward biased to provide gain. Electrical isolation between the electrodes was obtained by wet etching 10 μm wide and 200 nm deep slots in the contact layer. The laser fabrication process was similar to that described in [9]. As a final step, the sample was cleaved into individual laser bars with both facets left uncoated. The devices were mounted epilayer-up on a temperature controlled heat sink set at 20°C and tested under CW conditions.

3. Device performance

Figure 2 shows typical light-gain current (L-I_{Gain}) characteristics with different reverse bias values applied to the SA sections (V_{SA}) of the laser. The threshold current and single facet slope efficiency with the SA sections unbiased were 48 mA and 14.2% W/A, respectively. Increasing the V_{SA} increased the threshold current and reduced the slope efficiency as a result of the increased absorption. Kinks were observed when $|V_{SA}| > 1.5$ V. These are caused by thermal detuning between

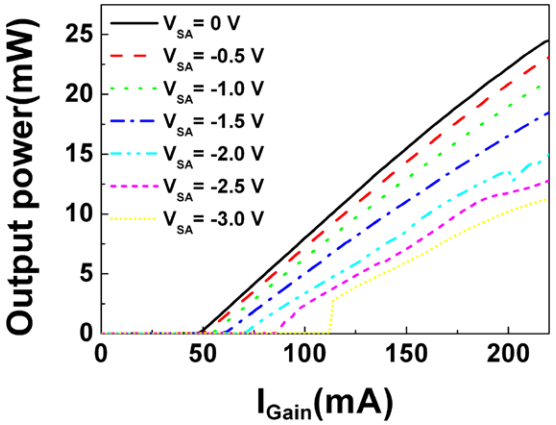

Figure 2. Typical L-I_{gain} characteristics at different values of V_{SA} from 0 to −3 V with an increment of −0.5 V.

the gain and SA sections and are associated with a longitudinal mode-hop (see figure 4). The α_i value for the epitaxial design was measured using the Hakki-Pauli method and was as low as ~8 cm^{-1} and the differential modal gain value was as low as ~2.7 × 10^{-17} cm^2 [9]. The divergence angles for the horizontal and vertical directions were 12.7° × 26.3° , respectively, while the measured butt coupling efficiency with a single-mode fibre (SMF) was about 20%, double that of a conventional MLL. The −1 dB alignment tolerances in the horizontal, vertical and optical axis have been significantly relaxed [9].

Passive ML of the device was achieved by forward biasing the gain sections and reverse biasing the SA sections. The purest sixth harmonic (i.e. ML frequency (F_r) of ~240 GHz with ~100% pulse modulation with a negligible pedestal), was obtained over a large SA bias range $-0.7 \le V_{SA} \le -1.9$ V and I_{Gain} range as denoted by the blue areas in figure 3(*a*). In these areas we observed optical spectra with the longitudinal modes lasing at every sixth mode with a spacing of ~240 GHz (figure 4), and a side-mode suppression ratio (SMSR) for the intermediate (non-lasing) modes at >30 dB. As noted, the wide 240 GHz pure ML range is attributed to the higher E_{sat} characteristics of the gain media and the fast absorption recovery times in AlGaInAs QWs, which has been measured to be <5 ps for an applied reverse bias above 3 V [10]. The ratio of E_{sat} between the gain and absorber media determines the range of stable ML [12]. The SA absorption recovery time determines the highest pure ML frequency achievable, and a recovery time <5 ps is sufficient for producing pure 240 GHz pedestal-free ML pulses [13].

An area of incomplete ML (IML) within the V_{SA} range from −0.3 V to −0.6 V is identified by the light grey grid area in figure 3(*a*), where the corresponding autocorrelation (AC) traces showed signs of a small pedestal (i.e. less than 100% pulse modulation). A ML region where the 240 GHz signal is modulated by a 40 GHz (i.e. the fundamental cavity length frequency) envelope is represented by the red grid area of figure 3(*a*), where the 240 GHz longitudinal modes had a SMSR value <20 dB at the central mode. All of these features can be directly linked to the optical longitudinal modal behavior displayed in figure 4.

From figure 3(*b*), it is clear that the measured full width at half maximum (FWHM) of the AC signal is very stable as I_{Gain} and V_{SA} are varied. The FWHM of the AC traces appear to be concentrated near values around 1.5 ps, which deconvolves

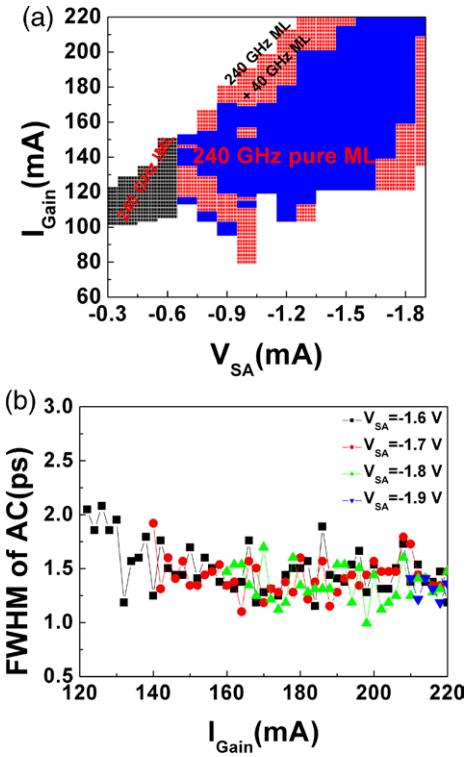

Figure 3. (*a*) Measured map of the ML regime as a function of I_{Gain} and V_{SA}, (*b*) FWHM of the AC traces versus I_{Gain} for V_{SA} = −1.6 to −1.9 V.

to a pulse duration of ~1 ps assuming a sech^2 pulse shape. This shows the pulse width of the 240 GHz CPM laser is very stable and insensitive to the applied bias conditions. This consistency in pulse width is a favorable feature of our MLLs, which confirms the laser is thermally and mechanically stable.

Figure 4 shows the wavelength map as a function of I_{Gain} for V_{SA} = −1.6 V to −1.9 V. In the pure ML range, the 240 GHz lasing modes are clearly observable with the longitudinal modes present at every sixth mode. The central mode has a SMSR of >30 dB. On the other hand, in the area characterized by 240 GHz ML modulated by 40 GHz ML, the SMSR of the central mode was <20 dB. Consistent with figure 2, longitudinal mode hopping occurs at the points where kinks are observed in the *L-I* curves. When V_{SA} was increased, the maximum I_{Gain} value for pure 240 GHz ML to occur was also increased, which is consistent with that shown in figure 3(*a*).

The laser output characteristics for I_{gain} = 220 mA and V_{SA} = −1.9 V are shown in figure 5. The average period of the measured emitted pulse train was 4.1 ps (figure 5(*a*)), corresponding to an F_r of 241 GHz. The autocorrelation width, τ, of an isolated pulse was 1.36 ps, which deconvolves to a 0.88 ps pulse duration Δt assuming a sech^2 pulse shape (figure 5(*b*)). The average output power was 15.7 mW, corresponding to a peak power of 65 mW.

The optical spectrum (measured with a 0.06 nm resolution bandwidth) was centered at 1570 nm with a −3 dB bandwidth of 3.95 nm. As noted, lasing of every sixth fundamental longitudinal mode occurred, and these were separated by ~241 GHz (figure 5(*c*)), consistent with the reciprocal of the

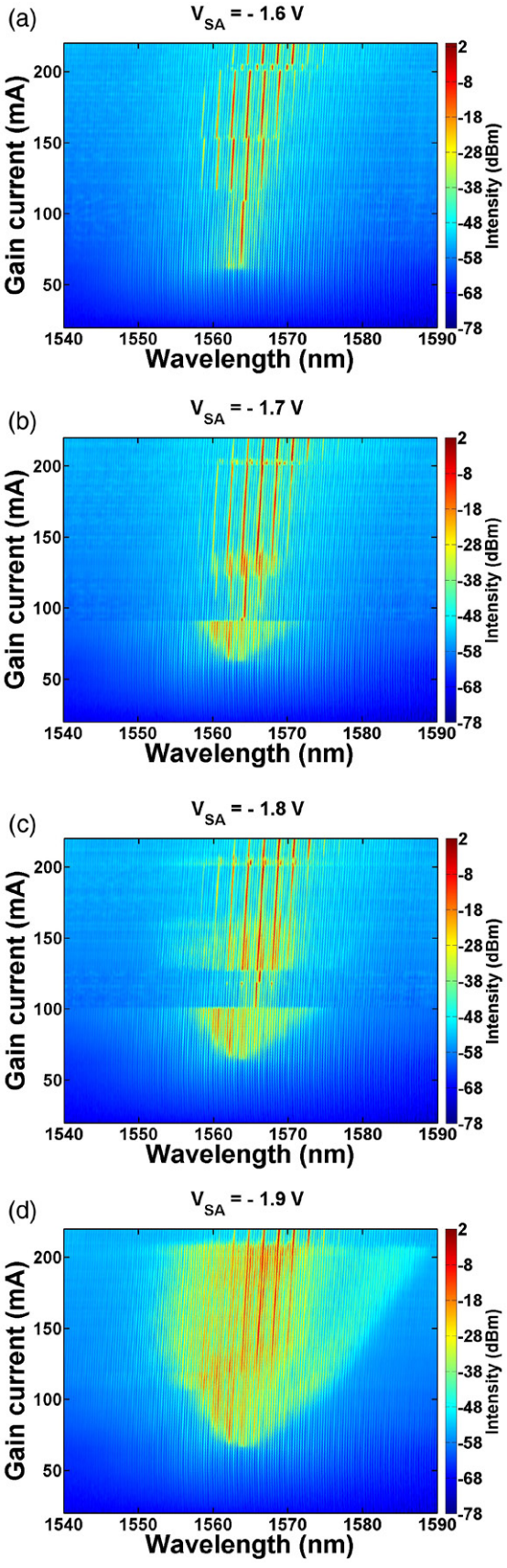

Figure 4. Wavelength map as a function of the I_{Gain} for V_{SA} = −1.6 V to −1.9 V.

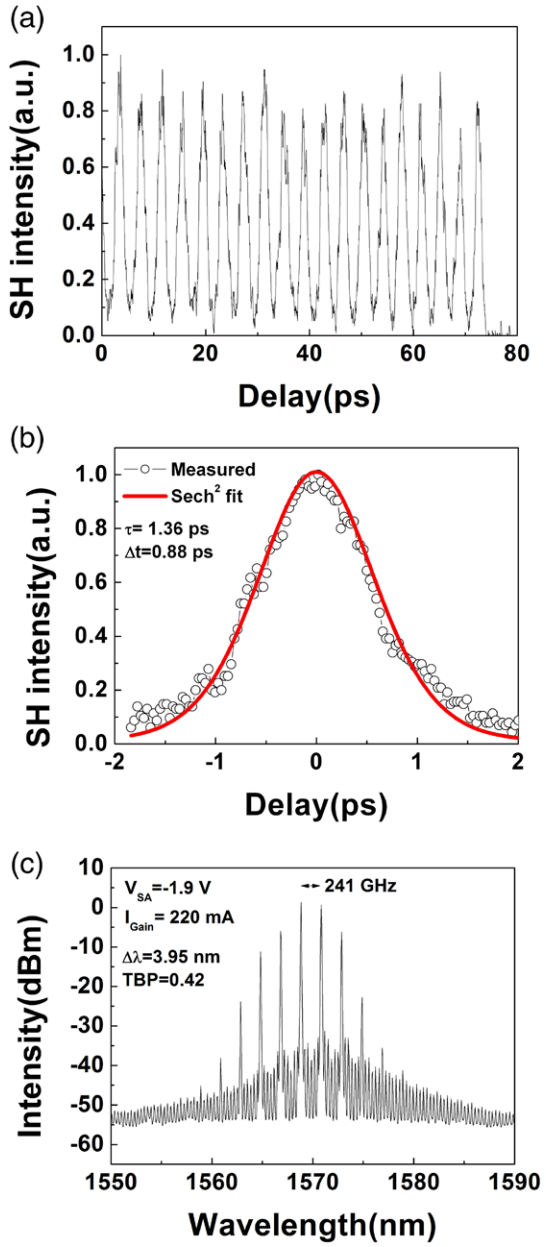

Figure 5. (*a*) Measured autocorrelation pulse train, (*b*) an isolated pulse fitted using a sech^2 profile, and (*c*) optical spectrum for I_{gain} = 220 mA and V_{SA} = −1.9 V.

pulse duration shown in figure 5(*a*), confirming the device was operating as a CPM laser at the sixth harmonic. The time-bandwidth product (TBP) of the pulse is equal to 0.42, which is somewhat larger than the transform-limited value (≈0.315) of a sech^2 waveform. This is likely to be due to the spectral broadening caused by SPM occurring mainly in the gain sections [11].

As anticipated, the equivalent laser fabricated using a five-QW Al-quaternary structure [14] with a Γ value of 5% resulted in a narrower harmonic ML range (figure 6(*a*)) and a lower average output power. Pure ML with ~100% modulation at ~240 GHz was obtained with V_{SA} = −2.0 V, 184 mA ≤ I_{gain} ≤ 196 mA. With V_{SA} = −2.0 V and I_{Gain} = 186 mA, the pulse width was 1.47 ps (figure 6(*c*)), the optical spectral 3 dB width was 3.49 nm (figure 6(*d*)), the mode spacing was 237 GHz which is consistent

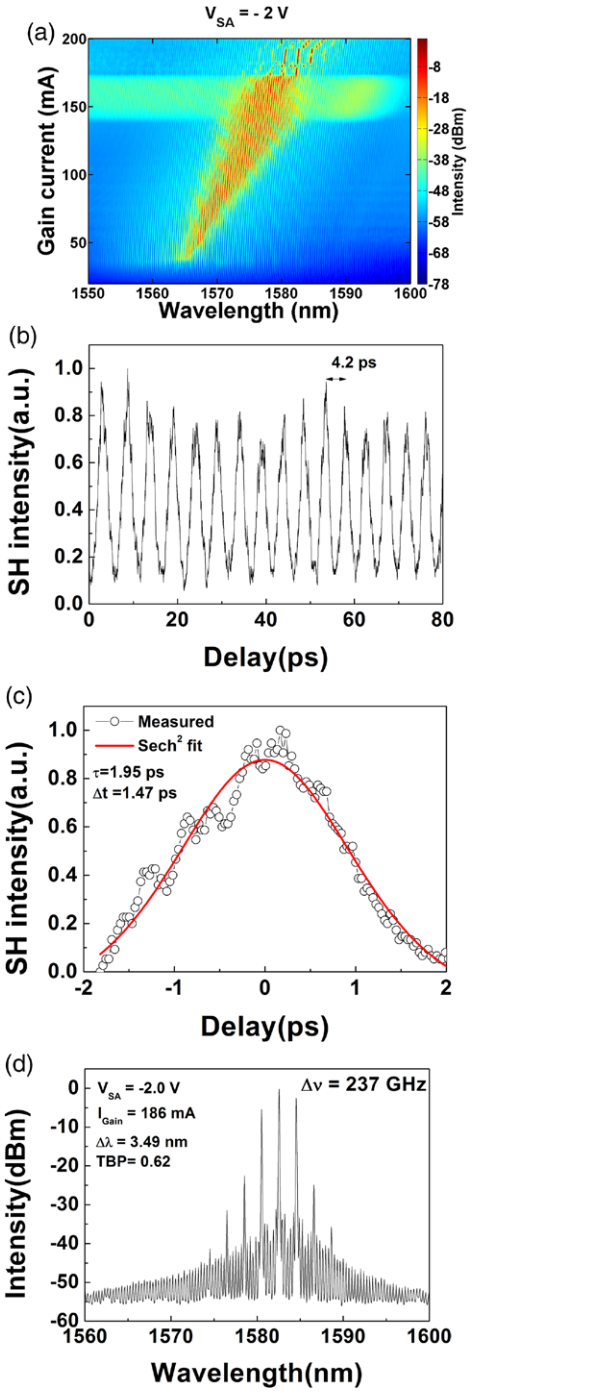

Figure 6. (*a*) Wavelength map as a function of the I_{Gain} for V_{SA} = −2.0 V for five-QW 240 GHz CPM laser, (*b*) measured autocorrelation pulse train, (*c*) an isolated pulse fitting by sech^2 shape, and (*d*) optical spectrum for I_{Gain} = 186 mA and V_{SA} = −2.0 V.

with the reciprocal of the average period of 4.2 ps shown in figure 6(*b*) and the TBP at 0.62. The average power was 11 mW and the peak power was ~28 mW, less than that of the three-QW laser with a FRL structure (65 mW).

4. Conclusions

In conclusion, we have reported an exceptionally wide ML operation range of a ~240 GHz CPM laser, passively

mode-locked at the sixth-harmonic of the fundamental cavity frequency. The device was based on a three-QW AlGaInAs epitaxial structure with a FRL design. Compared to equivalent devices based on conventional five-QW wafer designs, the device featured with a significantly improved ML range, FFP (12.7° × 26.3°), peak power (65 mW), and pulse duration (0.88 ps), and provided a twofold improvement in butt coupling efficiency to a flat cleaved SMF.

Acknowledgements

The authors would like to acknowledge financial support from EPSRC (project EP/E065112/1), and thank the technicians in the James Watt Nanofabrication Center, Glasgow.

References

[1] Sato K 2003 *IEEE J. Sel. Top. Quantum Electron.* **9** 1288–93
[2] Merghem K, Akrout A, Martinez A, Aubin G, Ramdane A, Lelarge F and Duan G H 2009 *Appl. Phys. Lett.* **94** 021107
[3] Chen Y, Wu M, Tanbun-Ek T, Logan R A and Chin M A 1991 *Appl. Phys. Lett.* **58** 1253–55
[4] Martins-Filho J F, Avrutin E A, Ironside C N and Roberts J S 1995 *IEEE J. Sel. Top. Quantum Electron.* **1** 539–51
[5] Katagiri Y and Takada A 1997 *IEEE Photon. Technol. Lett.* **9** 1442–4
[6] Hou L, Haji M, Dylewicz R, Stolarz P, Qiu B, Avrutin E and Bryce A C 2010 *Opt. Lett.* **35** 3991–3
[7] Yvind K, Larsson D, Christiansen L J, Angelo C, Oxenløwe L K, Mørk J, Birkedal D, Hvam J M and Hanberg J 2004 *IEEE Photon. Technol. Lett.* **16** 975–77
[8] Merghem K *et al* 2008 *Opt. Express* **16** 10675–83
[9] Hou L, Haji M, Akbar J, Qiu B C and Bryce A C 2011 *Opt. Lett.* **36** 966–8
[10] Green R P, Haji M, Hou L, Mezosi G, Dylewicz R and Kelly A E 2011 *Opt. Express* **19** 9737–43
[11] Agrawal G P and Olsson N A 1989 *IEEE J. Quantum Electron.* **25** 2297–306
[12] Haus H A 1975 *IEEE J. Quantum Electron* **QE-11** 736–46
[13] Karin J R, Helkey R J, Derickson D J, Nagarajan R, Allin D S, Bowers J E and Thornton R L 1994 *Appl. Phys. Lett.* **64** 676–8
[14] Hou L, Stolarz P, Javaloyes J, Green R, Ironside C, Sorel M and Bryce A C 2009 *IEEE Photon. Technol. Lett.* **21** 1731–3